

# New Method to Calculate Electrical Forces Acting on a Sphere in an Electrorheological Fluid

Kwangmo Kim and David Stroud<sup>y</sup>

Department of Physics, The Ohio State University, Columbus, Ohio 43210

Xiangting Li<sup>z</sup>

School of Physics and Astronomy, Raymond and Beverly Sackler Faculty of Exact Sciences,

Tel Aviv University, IL-69978 Tel Aviv,

Israel; and Institute of Theoretical Physics,

Shanghai Jiaotong University, Shanghai 200240, P.R. China

David J. Bergman<sup>x</sup>

School of Physics and Astronomy, Raymond and Beverly Sackler Faculty of Exact Sciences,

Tel Aviv University, IL-69978 Tel Aviv, Israel

(Dated: February 18, 2022)

## Abstract

We describe a method to calculate the electrical force acting on a sphere in a suspension of dielectric spheres in a host with a different dielectric constant, under the assumption that a spatially uniform electric field is applied. The method uses a spectral representation for the total electrostatic energy of the composite. The force is expressed as a certain gradient of this energy, which can be expressed in a closed analytic form rather than evaluated as a numerical derivative. The method is applicable even when both the spheres and the host have frequency-dependent dielectric functions and nonzero conductivities, provided the system is in the quasistatic regime. In principle, it includes all multipolar contributions to the force, and it can be used to calculate multi-body as well as pairwise forces. We also present several numerical examples, including host fluids with finite conductivities. The force between spheres approaches the dipole-dipole limit, as expected, at large separations, but departs drastically from that limit when the spheres are nearly in contact. The force may also change sign as a function of frequency when the host is a slightly conducting fluid.

---

Electronic address: kwangmoo@mps.ohio-state.edu

<sup>y</sup>Electronic address: stroud@mps.ohio-state.edu

<sup>z</sup>Electronic address: xtl@sjtu.edu.cn

<sup>x</sup>Electronic address: bergman@post.tau.ac.il

## I. INTRODUCTION

An electrorheological (ER) fluid is a material whose viscosity changes substantially with the application of an electric field [1]. Generally, such fluids are suspensions of spherical inclusions of dielectric constant  $\epsilon_i$  in a host fluid of a different dielectric constant  $\epsilon_h$ . The viscosity is believed to change because the spheres acquire electric moments (dipole and higher) when an electric field is applied, then move under the influence of the electrical forces between these induced moments. These forces typically cause the spheres to line up in long chains parallel to the applied field, thereby increasing the viscosity of the suspension. The viscosity relaxes to its usual value when the field is turned off, and the chain-like structure disappears.

ER fluids have potential applications as variable viscosity fluids in automobile devices [2], vibration control [3], and elsewhere. Furthermore, their operating principle is also relevant to other materials, such as magnetorheological (MR) fluids [4]. These are suspensions of magnetically permeable spheres in a fluid of different permeability, whose viscosity can be controlled by an applied magnetic field.

To obtain a quantitative theory of ER (and MR) fluids, one needs to understand the electric-field-induced force among the spheres. At low sphere concentrations and large inter-sphere separations, this force is just that between two interacting electric dipoles whose magnitude is that of a single sphere in an external electric field. But at smaller separations, the force deviates from the dipole-dipole form. Besides this electrostatic interaction between the spheres, there are other forces acting on the spheres, including a viscous frictional force from the host fluid, and a hard-sphere force when the two dielectric spheres come in contact. In the present paper, we will be concerned only with the electrostatic force.

A number of existing theories go beyond the dipole-dipole approximation in calculating electrostatic forces in ER fluids [5, 6, 7, 8, 9, 10, 11, 12, 13], and several experiments have been carried out which are relevant to forces in the non-dipole regime (see, e. g., Refs. [14, 15]). Klingenberg et al. [5] have incorporated both multipole and multi-body effects into the sphere-sphere interactions, using a perturbation analysis. Chen et al. [6] have described a multipole expansion for the forces acting on one sphere in a chain of spheres in a fluid of different dielectric constant, and find a strong departure from the dipolar limit when the particles are closer than about one diameter. Davis [7] has calculated the electrostatic forces

between dielectric spheres in a host fluid directly, using a finite element approach to solve Laplace's equation for a chain of particles in a host dielectric. In a more recent work [8], he has used an integral equation approach to calculate the interparticle forces in ER fluids, including effects due to time-dependent application of an external field, and nonlinear fluid conductivity. A finite element approach has also been used by Tao et al. [9] to solve Laplace's equation and obtain the electrostatic interactions between particles in a chain of dielectric spheres in a host fluid; they found, as in Ref. [7], that the dipole-dipole approximation is reasonably accurate for large separations or moderate dielectric mismatches, but fails in closely spaced particles and large mismatches. Clercx and Bossis [13] have gone beyond the approximation of dipolar interactions to include multipolar and many-body interactions, expressed in terms of the induced multipole moments on each sphere; they also obtain an expression for the forces in terms of these induced multipole moments.

As discussed further below, the electrical force acting on a sphere in an electrorheological fluid is basically the gradient of the total electrostatic energy of that fluid with respect to the position of the sphere. This total electrostatic energy can, in turn, be expressed in terms of the effective dielectric tensor of the suspension, a quantity which has been studied since the time of Maxwell. Indeed, numerous authors have calculated this tensor in a wide variety of geometries, going well beyond the regime of purely dipolar interactions. For example, Jeffrey [16] has calculated the total energy of two spheres in a suspension as a function of their separation and the dielectric mismatch. From this total energy, the force can be obtained numerically as the derivative of this energy with respect to separation. Recently, the pairwise forces between spheres of different sizes have been calculated using the so-called dipole-induced-dipole approximation, and even approximately including the effects of other spheres [17]. Once again, the forces were obtained explicitly by numerically differentiating the total electrostatic energy with respect to particle coordinates. McPhedran and McKenzie [18], and Suen et al. [19], and many others, have calculated the total energy of spheres arranged in a periodic structure. In principle, forces could also be extracted from this calculation by taking numerical derivatives, provided that the distortions of the structure leave it periodic. The energy of a non-periodic suspension of many spheres has been studied by Gerardy and Ausloos [20] and by Fu et al. [21], in both cases including large numbers of multipoles. Once again, forces can be extracted, in principle, from these calculations by taking numerical derivatives of the computed total energies with respect to

sphere coordinates.

Several authors have included the effects of finite conductivity on forces in electrorheological fluids, and have also considered how such forces depend on frequency. Davis[22] has analyzed polarization forces and related effects of conductivity in ER fluids. Tang et al.[10, 11] have calculated the attractive force between spherical dielectric particles in a conducting fluid. Khusid and Acrivos[12] have considered electric-field-induced aggregation in ER fluids, including interfacial polarization of the particles, the conductivities of both the particles and the host fluid, and dynamics arising from dielectric relaxation. Claro and Rojas[23] have calculated the frequency-dependent interaction energy of polarizable particles in the presence of an applied laser field within the dipole approximation; they considered primarily optical frequencies rather than the low frequencies more characteristic of ER fluids. Ma et al.[24] have considered several frequency-dependent properties of ER systems, starting from a well-known spectral representation [25, 26, 27, 28, 29, 30] for the dielectric function of a two-component composite medium. Finally, Huang[31] has carried out a calculation of the force acting in electrorheological solids under the application of a non-uniform electric field, and considering both finite frequency and finite conductivity effects.

A common feature of most of the above approaches is that they involve first calculating the total electrostatic energy of the suspensions, then obtaining the forces by numerically differentiating this energy with respect to a particle coordinate. This numerical differentiation is cumbersome and can be inaccurate. Ref. [13] does give an expression for the force, but in terms of implicitly defined multipoles. In this paper, by contrast, we describe a method for calculating these forces explicitly, without numerical differentiation. This approach is computationally much more accurate than numerically differentiating the energy. While our new method may appear to be merely a computational advance, its additional accuracy and flexibility should make it widely applicable.

Specifically, our approach allows one to calculate the electric-field-induced force between two dielectric spheres in a host of a different dielectric constant, at any separation. It is applicable, in principle, to spheres of unequal sizes, to particles of shape other than spheres, to suspensions in which either the particle or the host or both have nonzero conductivities, and to systems whose constituents have frequency-dependent complex dielectric functions. It can also be used to calculate the electrostatic force on one particle which is part of a many-particle system, and thus is not limited to two-body interaction. It should thus be

useful in quite general circumstances including, in particular, non-dilute suspensions.

Our approach starts, as do previous calculations, with a method for calculating the total electrostatic energy of a suspension of (two or more) spheres in a host material of different dielectric constant. We choose to express this total energy in terms of a certain pole spectrum arising from the quasistatic resonances of the multi-sphere system [25, 26, 27, 28, 29, 30]. This representation has previously been used to calculate the frequency-dependent shear modulus, static yield stress, and structures of certain ER systems [24, 32, 33, 34]. The force on a given sphere in a multi-sphere system involves a gradient of this energy with respect to the position of that sphere. But rather than evaluating this derivative numerically, as in previous work [24], we express this derivative in closed analytical form in terms of the pole spectrum and certain matrix elements involving the resonances. This expression is readily evaluated simply by diagonalizing a certain matrix, all of whose components are readily computed.

Our approach has formal similarities to the well-known Hellmann-Feynman expression for forces in quantum-mechanical systems [35]. In the quantum-mechanical case, the force is expressed as the negative gradient of system energy with respect to an ionic position. This energy is the expectation value of the Hamiltonian in the ground state. According to the Hellmann-Feynman theorem, the gradient operator can be moved inside the matrix element, thereby eliminating the need to take numerical derivatives. The Hellmann-Feynman force expression is the basis for many highly successful molecular dynamics studies in quantum systems (see, e. g., Ref. [36]). In the present classical case, the total energy can also be expressed as a certain matrix element of an operator, and thus, just as in the quantum problem, the force is the gradient of that expectation value. In this paper, we shall show that, again as in the quantum case, the gradient operator can be moved to within the matrix element, and the need to take a numerical derivative is eliminated. This simplification allows, in principle, the calculation of forces in very complicated geometries, even though, in the present paper we shall give only relatively simple numerical illustrations involving forces between two spherical particles.

The remainder of this paper is organized as follows. In Section II, we present the formalism necessary to calculate the forces in a system of two or more dielectric spheres in a host medium, without taking a numerical derivative. In Section III, we give several numerical examples of these forces, at both zero and finite frequencies, for a two-sphere system.

Section IV presents a concluding discussion and suggestions for future work.

## II. FORMALISM

Let us assume that we have a composite consisting of spherical inclusions of isotropic dielectric constant  $\epsilon_i$  in a host of isotropic dielectric constant  $\epsilon_h$ , both of which may be complex and frequency-dependent. We will assume that a spatially uniform electric field  $\text{Re}[E_0 e^{i\omega t}]$  is applied in an arbitrary direction (we take  $E_0$  real). We also assume that the system is in the "quasistatic regime." In this regime, the product  $k a \ll 1$ , where  $k$  is the wave vector and  $a$  is a characteristic length scale describing the spatial variation of  $\phi(\mathbf{x}; \omega)$ . Under these conditions, the local electric field  $E(\mathbf{x}; \omega) = -\nabla \phi$ , where  $\phi$  is the electrostatic potential. Finally, we assume that the  $R^{\text{th}}$  spherical inclusion is centered at  $\mathbf{R}$ , and has radius  $a_R$ . The approach which we use automatically includes all local field effects.

Since our force expressions differ slightly at zero and finite frequencies, we will first present the formalism at  $\omega = 0$ , and then generalize the results to finite  $\omega$ .

### A. Zero Frequency

If the position of the spheres is fixed, the total electrostatic energy may be written in the form

$$W = \frac{V}{8} \sum_{i=1}^N \sum_{j=1}^N \epsilon_{ij} E_{0i} E_{0j}; \quad (1)$$

where  $V$  is the system volume,  $\epsilon_{ij}$  is a component of the macroscopic effective dielectric tensor, and  $E_{0i}$  is a component of the applied electric field. Eq. (1) is, in fact, a possible definition of  $\epsilon_{ij}(\omega)$  [28]. To produce this applied field, we require that  $\phi(\mathbf{x}) = -E_0 x$  at the boundary  $S$  of the system, which is assumed to be a closed surface enclosing  $V$ . In writing eq. (1), we allow for the possibility that the spheres in the composite are arranged in such a way that the composite is anisotropic even though its components are not.

For an isotropic composite,  $\epsilon_e$  may be written in terms of a certain pole spectrum of the composite as [25, 26, 27, 28, 29, 30]

$$1 - \frac{\epsilon_e}{\epsilon_h} = \sum_s \frac{B_s}{s - \omega^2}; \quad (2)$$

where

$$s = \frac{1}{1 - \frac{\epsilon_h}{\epsilon_i}}; \quad (3)$$

$s$  is a pole, and  $B$  is the corresponding residue. The poles  $s$  are confined to the interval  $0 < s < 1$ . For an anisotropic composite, this form may be generalized to

$$\epsilon_{ij} = \epsilon_h + \sum_s \frac{B_{ij}}{s - s_j}; \quad (4)$$

where  $\delta_{ij}$  is a Kronecker delta function and  $B_{ij}$  is a matrix of residues. This form is general, applicable to any two-component composite material which is made up of isotropic constituents, but is not necessarily isotropic macroscopically. As in the isotropic case, the poles are confined to the interval  $0 < s < 1$ .

The poles  $s$  are the eigenvalues of a certain Hermitian operator  $\hat{S}$ , and the residues  $B$  are determined by the eigenvectors of that operator.  $\hat{S}$  is defined in terms of its operation on an arbitrary function  $\phi(r)$  by the relation

$$(\hat{S}\phi)(r) = \frac{1}{V_{\text{tot}}} \int_{V_{\text{tot}}} d^3r' \phi(r') \epsilon(r, r'); \quad (5)$$

where the integration runs over the total volume  $V_{\text{tot}}$  of all the inclusions of  $\epsilon_i$ . As in Ref. [37], we introduce a "bra-ket" notation for two potential functions to denote their inner product,

$$(\phi | \psi) = \frac{1}{V_{\text{tot}}} \int_{V_{\text{tot}}} d^3r \phi(r) \psi(r); \quad (6)$$

Physically, the eigenvalues correspond to the frequencies of the natural electrostatic modes of the composites, at which charge can oscillate without any applied field, and the corresponding eigenvectors describe the electric fields of those modes.

It is convenient to express  $\hat{S}$  in terms of its matrix elements between the normalized eigenstates of isolated spheres. In this basis, and using eqs. (5) and (6), it is found that  $\hat{S}$  has the following matrix elements:

$$S_{R\gamma m, R'\gamma' m'} = \delta_{R\gamma m, R'\gamma' m'} s_{R\gamma m} + Q_{R\gamma m, R'\gamma' m'} (1 - s_{R\gamma m}); \quad (7)$$

where  $s_{R\gamma m}$  and  $Q_{R\gamma m, R'\gamma' m'}$  will be given further below. Inside the sphere centered at  $R$ ,  $\psi_{R\gamma m}(r)$  is equal to an eigenfunction or resonance state of that isolated sphere, while outside that sphere  $\psi_{R\gamma m}(r) = 0$ . The angular dependence of  $\psi_{R\gamma m}(r)$  is given by the spherical harmonic  $Y_{\gamma m}(\theta, \phi)$ , which has an order  $\gamma$  multipole moment of electric polarization. However, the eigenvalue of this state depends only on  $\gamma$ :

$$s_{R\gamma m} = s_{\gamma} = \frac{\gamma}{2\gamma + 1}; \quad (8)$$



The quantity  $Q_{R^0 m^0 R^0 m^0}$  represents the matrix element of  $\hat{Q}$  between two states of two different, non-overlapping spheres (i.e.,  $R^0 \neq R^0$ ) and is given by

$$Q_{R^0 m^0 R^0 m^0} = (-1)^{m^0} \frac{a_{R^0}^{l+1=2} a_{R^0}^{l+1=2}}{R^0 R^0} \frac{1}{(2l+1)(2l+1)} \frac{1}{(l+m^0)!} \frac{1}{[(l+m^0)!(l-m^0)!(l+m^0)!(l-m^0)!]^{1/2}} e^{i R^0 R^0} P_{l+m^0}^{m^0}(\cos R^0 R^0); \quad (9)$$

where  $R^0 R^0$  and  $R^0 R^0$  are polar and azimuthal angles of the vector  $R^0 R^0$ , and the functions  $P_{l+m^0}^{m^0}$  are the associated Legendre polynomials.

If we denote the eigenfunctions of  $\hat{Q}$  by  $\psi_j(r)$ , then  $s_j$  and  $\psi_j(r)$  satisfy the eigenvalue equation

$$\hat{Q} \psi_j = s_j \psi_j; \quad (10)$$

Since  $\hat{Q}$  is a Hermitian operator, the eigenvalues  $s_j$  are real, and the corresponding eigenfunctions are orthogonal and can be chosen to be orthonormal. Again, it is convenient to represent them using a bra-ket notation. In this notation, the eigenfunctions are denoted  $|j\rangle$  and the orthonormality condition is

$$\langle j | i \rangle = \delta_{ji}; \quad (11)$$

The eigenvalues  $s_j$  are the poles of eq. (2) or eq. (4).

The corresponding residues  $B_{ji}$  may be expressed in the same bra-ket notation as

$$B_{ji} = \frac{V_{tot}}{V} \langle j | \hat{Q} | i \rangle \langle i | i \rangle = M^i M^j; \quad (12)$$

The matrix element  $M^i = \langle j | \hat{Q} | i \rangle$  is basically the component of the electric dipole moment of the eigenfunction  $|j\rangle$  in the  $i^{th}$  Cartesian direction.

It is convenient to expand both the eigenfunctions  $|j\rangle$  and the states  $|ji\rangle$  ( $i = x, y, z$ ), in terms of the single-sphere eigenfunctions  $\psi_{R^0 m^0}(r)$  mentioned above. In bra-ket notation,

$$|j\rangle = \sum_{R^0 m^0} A_{R^0 m^0} |j R^0 m^0\rangle; \quad (13)$$

The expansion coefficients satisfy the normalization condition  $\sum_{R^0 m^0} |A_{R^0 m^0}|^2 = 1$ , where the indices  $l = 1, 2, \dots$  and  $m = -l, \dots, +l$  respectively. Similarly, the states  $|ji\rangle$  may be expanded as

$$|ji\rangle = \sum_{R^0 m^0} M_{R^0 m^0}^i |j R^0 m^0\rangle; \quad (14)$$

where  $i = x, y, z$ . If the  $z$  axis is chosen as the polar axis for the spherical harmonics, then the  $M_{R\gamma m}^i$  take the form [26]

$$\begin{aligned} M_{R\gamma m}^x &= \frac{v_R}{2v_{\text{tot}}} \frac{1=2}{\gamma=1} (m;1 + m;-1) \gamma=1; \\ M_{R\gamma m}^y &= i \frac{v_R}{2v_{\text{tot}}} \frac{1=2}{\gamma=1} (m;1 - m;-1) \gamma=1; \\ M_{R\gamma m}^z &= \frac{v_R}{v_{\text{tot}}} \frac{1=2}{\gamma=1} m;0 \gamma=1; \end{aligned} \quad (15)$$

Thus, the matrix elements  $M^i$  are given explicitly by

$$\begin{aligned} M^x &= \sum_R \frac{v_R}{2V} \frac{1=2}{\gamma=1} (A_{R11} + A_{R1-1}); \\ M^y &= i \sum_R \frac{v_R}{2V} \frac{1=2}{\gamma=1} (A_{R11} - A_{R1-1}); \\ M^z &= \sum_R \frac{v_R}{V} \frac{1=2}{\gamma=1} A_{R10}; \end{aligned} \quad (16)$$

In other words, the residues of the  $i^{\text{th}}$  eigenfunction are basically the square of the electric dipole moment of that mode in the  $x$ ,  $y$ , or  $z$  direction.

Combining these results, we can re-express the matrix elements (4) of the dielectric tensor in bra-ket notation first as

$$\epsilon_{ij} = \frac{v_{\text{tot}}}{V} \sum_h \frac{h_{ij} h_{ji}}{s}; \quad (17)$$

where the explicit forms of  $h_{ij}$  and  $h_{ji}$  are given by eqs. (16).

We now use the above formalism to obtain an expression for the force on a dielectric sphere centered at  $R$  in a suspension consisting of an arbitrary assembly of spheres. First, we rewrite eq. (17) as

$$\epsilon_{ij} = \frac{v_{\text{tot}}}{V} \sum_h h_{ij} G(s) h_{ji}; \quad (18)$$

where

$$G(s) = \sum_j \frac{j_{ih} j_{jh}}{s} = (sI)^{-1}; \quad (19)$$

is a Green's function for this problem,  $I$  is the identity matrix, and the matrix elements of are given by eq. (7). If the applied electric field is  $E_0$ , the total energy takes the form

$$W = \frac{V}{8} \sum_h E_0 \cdot \epsilon_{ij} \frac{v_{\text{tot}}}{V} \sum_h E_{0,i} h_{ij} G(s) h_{ji} E_{0,j}; \quad (20)$$

We now write the  $k^{\text{th}}$  component of the force on the sphere at  $R$  as

$$F_{R_k} = + \frac{\partial W}{\partial R_k} \quad (21)$$

Here  $R_k$  denotes the  $k^{\text{th}}$  component of  $R$ , and the subscript denotes that the derivative is taken with the potential fixed on the boundaries. The positive sign, though seemingly counterintuitive, is actually correct here because the system is held at fixed potential on the boundaries[38]. Using eq. (20), the derivative in eq. (21) can be expressed as

$$\frac{\partial W}{\partial R_k} = \frac{v_{\text{tot}}}{8} \sum_{ij} E_{0;i} E_{0;j} \text{tr} \left[ \frac{\partial}{\partial R_k} G(s) \right]_{ji} \quad (22)$$

The derivative can be brought inside the bras and kets because these bras and kets do not depend on  $R_k$ .

The derivative of  $G(s)$  appearing in eq. (22) can be evaluated straightforwardly. Let us assume that the operator depends on some scalar parameter (e.g.,  $R_k$ ). Then, if we introduce the operator  $U = \partial / \partial$ , we can calculate the partial derivative  $\partial G(s; ) / \partial$  as follows:

$$\begin{aligned} \frac{\partial G(s; )}{\partial} &= \lim_{\epsilon \rightarrow 0} \frac{1}{\epsilon} \left( \text{tr} [sI - \epsilon U G(s; )] - \text{tr} [sI - \epsilon U G(s; )] \right) = \lim_{\epsilon \rightarrow 0} \frac{1}{\epsilon} \left( \text{tr} [sI - \epsilon U G(s; )] - \text{tr} [sI - \epsilon U G(s; )] \right) \\ &= \lim_{\epsilon \rightarrow 0} \frac{1}{\epsilon} \left( \text{tr} [sI - \epsilon U G(s; )] - \text{tr} [sI - \epsilon U G(s; )] \right) = \lim_{\epsilon \rightarrow 0} \frac{1}{\epsilon} \left( \text{tr} [sI - \epsilon U G(s; )] - \text{tr} [sI - \epsilon U G(s; )] \right) \\ &= \text{tr} [sI - \epsilon U G(s; )] - \text{tr} [sI - \epsilon U G(s; )] \\ &= G(s; ) U G(s; ) \end{aligned} \quad (23)$$

We can now use the above identity to calculate the force as given in eqs. (21) and (22). The result is

$$F_{R_k} = \frac{v_{\text{tot}}}{8} \sum_{ij} E_{0;i} E_{0;j} \text{tr} \left[ G(s; ) U_{R_k} G(s; ) \right]_{ji} \quad (24)$$

where we have introduced

$$U_{R_k} = \frac{\partial}{\partial R_k} \quad (25)$$

Using the representation (19) for  $G(s; )$  [and taking the eigenvalue  $s$  and the eigenstate  $j$  to refer to the operator  $(R_k)$ ], we can rewrite eq. (24) as

$$F_{R_k} = \frac{v_{\text{tot}}}{8} \sum_{ij} E_{0;i} E_{0;j} \sum_{s, s'} \frac{\langle j | U_{R_k} | j \rangle}{(s - s') (s - s')} \quad (26)$$

Eq. (26) is our central formal result.

As noted earlier, eq. (22) bears a resemblance to the Hellmann-Feynman theorem in quantum mechanics[35]: in both cases, the derivative of an operator with respect to a parameter appears inside a matrix element. But there is a significant difference between the two. In the Hellmann-Feynman case, the ket which plays the role of  $|j\rangle$  is an eigenstate of an operator, which is the actual Hamiltonian of the system. Although the ket in that case depends on  $\lambda$ , the derivative can still be moved inside the bra and ket because the eigenstates are orthonormalized. Here, by contrast, the states  $|j\rangle$  and  $|i\rangle$  are not eigenstates of the operator  $\hat{U}_{R_k}$ , but they do not depend on  $R_k$ ; so the derivative can still be moved inside the matrix element. This simplification allows forces to be computed without carrying out numerical derivatives.

Eq. (26) may appear to be rather difficult to apply in practice. But in fact it is computationally quite tractable. Basically, there are two matrices which are needed as inputs:  $G$  and  $U_{R_k} = \partial \mathcal{E} / \partial R_k$ .  $G$  is diagonal in the same basis as  $\hat{U}_{R_k}$ . All the matrix elements of  $\hat{U}_{R_k}$  are explicitly known in the  $R_k$  basis [cf. eq. (7)]. Likewise, the matrix elements of  $\partial \mathcal{E} / \partial R_k$  can be obtained from  $\mathcal{E}$  purely by elementary calculus. Thus, in order to compute the force component  $F_{R_k}$ , one first finds the eigenvalues and eigenfunctions of  $\hat{U}_{R_k}$  (and hence of  $G$ ), then computes the matrix  $G U_{R_k} G$  in the basis in which  $\hat{U}_{R_k}$  is diagonal, and finally the matrix elements  $\langle i | G U_{R_k} G | j \rangle$ , from which the force can be computed for any direction of the applied field  $E_0$ . Since the diagonalization can be done with standard computer packages, the whole procedure is well defined and straightforward. Furthermore, once  $\hat{U}_{R_k}$  has been diagonalized, the same basis can be used to compute the forces for any value of the variable  $s = (1 - \epsilon_i / \epsilon_h)^{-1}$ .

To illustrate how this formalism can actually be used to compute the force explicitly, we will consider just a suspension of two spheres, the two spheres being located at  $(0;0;0)$  and  $(0;0;R_0)$ . The total energy is given by eq. (1). We consider two configurations for the electric field:  $E_0 = (0;0;E_0)$  (we call this the "parallel configuration") and  $E_0 = (E_0;0;0)$  ("perpendicular configuration"). In both cases, the component of the force on the sphere at  $R_0$  along the axis joining the two spheres can be calculated using eq. (26).

To compute the force explicitly in this example, we have to consider how the operator changes with the separation  $R_0$  of the spheres, so that we can compute the matrix elements of  $U_{R_0}$ . According to eqs. (7) and (9), the diagonal matrix elements of  $\hat{U}_{R_0}$  are independent of  $R_0$ , while each of the off-diagonal matrix elements, according to eq. (9), is proportional to an

integer power of  $1/R^0 - R^j - 1/R_0$ . Hence,  $U_{R_0} @ = @R_0$  is easily calculated in a closed form. For the case of two spheres, it is straightforward to calculate this derivative. The eigenstates  $j_i$ , as well as  $s$ , are already known if the original eigenvalue problem involving  $(R_0)$  has been solved. The kets  $j_i$  are given by eq. (15). Therefore, it is straightforward to calculate the quantity  $\langle j_{R_0} | j_i \rangle$  and hence the force, using eq. (26).

### B. Finite Frequencies

The results of the previous subsection are readily generalized to finite frequencies. In this case, the total electrostatic energy will be a sinusoidally varying function of time. The quantities of experimental interest will be the time-averaged electrostatic energy  $W_{av}$  and time-averaged forces.  $W_{av}$  is given by the generalization of eq. (1), with an extra factor of  $1/2$  to take into account time-averaging, namely

$$W_{av} = \frac{V}{16} \text{Re} \sum_{i=1}^2 \sum_{j=1}^3 e_{ij}(\omega) E_{0,i} E_{0,j}^* \quad (27)$$

Here the applied field is assumed to be  $E_0 \cos(\omega t) = \text{Re}[E_0 e^{i\omega t}]$ ,  $e_{ij}(\omega)$  is a component of the complex frequency-dependent macroscopic effective dielectric tensor, and  $E_0$  is a real vector. All the remaining equations in Sec. IIA continue to be valid up to eq. (21), which is replaced by

$$F_{av,R_k} = + \frac{\partial W_{av}}{\partial R_k} \omega \quad (28)$$

where  $\omega$  is held fixed. The generalization of eq. (26) is

$$F_{av,R_k} = \text{Re} \sum_{i=1}^2 \sum_{j=1}^3 \frac{V_{tot,h}}{16} E_{0,i} E_{0,j}^* \frac{\langle j_{R_k} | j_i \rangle \langle j_i | j_5 \rangle}{(s_i - s)(s_j - s)} \quad (29)$$

Expression (29) can be evaluated just as at  $\omega = 0$ , and thus the time-averaged force at finite frequency can also be computed explicitly.

## III. NUMERICAL RESULTS

We have applied the above formalism to two spheres of dielectric constant  $\epsilon_i$  in a host of dielectric constant  $\epsilon_h$ . In most cases, we assume that the spheres have the same radius. We choose a coordinate system such that the two spheres are located at the origin and at  $R = R\hat{z}$ , and we consider two configurations for the applied electric field,  $E_0 = E_0\hat{z}$  and  $E_0 = E_0\hat{x}$ , as shown in Fig. 1.

Once the elements of the  $\mathbf{Q}$  and  $\mathbf{U}_R$  matrices are known, the calculation of the interparticle force reduces to an eigenvalue problem. To carry out the various required matrix and vector operations, we used GNU Scientific Library (GSL) routines[39] and C++ complex class library. In the parallel configuration, we calculated all the elements in the  $\mathbf{Q}$  and  $\mathbf{U}_R$  matrices up to  $l_{\max} = 80$ ; it is easy to include such a large cutoff because only  $m = 0$  needs to be considered for this geometry, the polar and azimuthal angles of  $\mathbf{R}$  equaling zero. Despite the large cutoff, most of the contributions to these matrices came from  $l < 10$ . Based on this information, we set  $l_{\max} = 10$  for the  $\mathbf{Q}$  and  $\mathbf{U}_R$  matrices in the perpendicular geometry. Even with this cutoff, the matrices involved in this calculation are large since  $m$  can be nonzero in the perpendicular case: the dimension of the matrix for  $l \leq 10$  is  $2^{l+1} (2l+1) = 240$ .

The matrix for both cases consists of four square blocks. The two diagonal square blocks have diagonal elements  $s_l = l(l+1)$  with all off-diagonal elements vanishing. The other two (off-diagonal) square blocks have elements  $Q_{lm,R}^{lm,0}$ . For the  $\mathbf{U}_R$  matrix, the diagonal square blocks have all zero elements, and the elements of the two off-diagonal blocks are equal to  $Q_{lm,R}^{lm,0} = Q_R$ . Once we have calculated all the eigenvalues and eigenvectors of the matrix, we can compute the  $\mathbf{M}$ ,  $\mathbf{B}$ , and hence the force on the sphere from  $\mathbf{h} \cdot \mathbf{j}_R$ , using eq. (26) or (29).

As a first example, we have considered  $\epsilon_i = 10^5$ ,  $\epsilon_h = 1$ . The choice for  $\epsilon_i$  approximates the value  $\epsilon_i = 1$  corresponding to two metallic spheres at zero frequency in an insulating host with unit dielectric constant. In Fig. 2, we show the magnitude of the calculated radial component of the force acting on the sphere at  $R$ , as a function of the sphere separation, for both parallel and perpendicular configurations. Although not apparent from the plot, this component of the force is attractive (i.e., negative) in the parallel configuration, repulsive in the perpendicular configuration. We have arbitrarily chosen sphere radii of  $a = 3.15$  nm and a field strength of  $E_0 = 25.2$  V/nm as in recent experiments carried out in Ref. [15] (for different materials). However, the forces are easily scaled with both field strength and sphere radii: for fixed  $\epsilon_i$  and  $\epsilon_h$  the appropriate scaling relation is

$$F_{12}^{i,k} = a^6 E_0^2 f_{i,k}(\epsilon_i; \epsilon_h; R/a); \quad (30)$$

where  $f_i$  and  $f_k$  are functions of  $\epsilon_i$ ,  $\epsilon_h$  and the ratio  $R/a$ .

It is of interest to compare these plots with the same forces as calculated in the dipole-dipole approximation. For two parallel dipoles  $p_1$  and  $p_2$ , located at the origin and at

$R = R \hat{z}$ , the  $z$  component of the force acting on the sphere at  $R$  has the well-known form

$$F_{12}^{\text{dip},k}(R) = 3 \frac{p_1 p_2}{R^4} \hat{p}_1 \cdot \hat{z}; \quad (31)$$

where  $p_1$  and  $p_2$  are the magnitudes of the two dipole moments, and  $\hat{p}_1$  is a unit vector parallel to  $p_1$  (or  $p_2$ ). For the present case, if the spheres are well separated and have equal radii, the dipole moments can be calculated as if each is an isolated sphere in a uniform external electric field  $E_0$ :

$$p_1 = p_2 = a^3 E_0 \frac{1}{1 + 2}; \quad (32)$$

For the cases in which the unit vector  $\hat{E}_0$  is perpendicular and parallel to  $\hat{z}$ , the radial component of the force reduces to

$$F_{12}^{\text{dip},\perp} = \frac{1}{2} F_{12}^{\text{dip},k} = 3 a^6 E_0^2 \frac{1}{1 + 2} \frac{1}{R^4}; \quad (33)$$

These values of  $F_{12}^{\text{dip},\perp}$  and  $F_{12}^{\text{dip},k}$  shown in Fig. 2 agree very well with those calculated from eq. (33) (taking  $\epsilon_i = 1$ ) at large separation ( $R \gg a$ ) but depart strongly at small separation ( $R \approx 2a$ ). Just as in the exact calculation, the radial component of the force in the dipole-dipole limit is repulsive in the perpendicular case and attractive in the parallel case. However, the ratio of the two forces in the parallel and perpendicular configurations at small separation has a magnitude greater than 50 for  $R = 0.632 \text{ cm} = 2a + 0.002 \text{ cm}$ , which is much larger than the factor of 2 expected from the dipole-dipole approximation. Further examples of this ratio are given in Table I for various separations.

In Figs. 3 and 4, we test the effect of different inclusion dielectric constants, by calculating the force between two identical spheres, each of radius  $a$  and dielectric constant  $\epsilon_i$ , in a host of dielectric constant  $\epsilon_h = 1$ . We plot the radial component of this force, for both the parallel and perpendicular configurations, as a function of  $\epsilon_i$ , for two different separations between the spheres:  $R = 2a + 0.01 \text{ mm}$  and  $R = 2a + 10.00 \text{ mm}$ , where we again use  $a = 3.15 \text{ mm}$ . In the second case, the forces are very close to the dipole-dipole predictions. In the first case, the forces exhibit a large departure from the predictions of the dipole-dipole interaction, and this departure becomes greater as  $\epsilon_i$  deviates more and more from unity.

Next, we consider an example in which the dielectric functions of both the inclusion and the host depend on frequency. Specifically, we choose

$$\epsilon_i = \epsilon_0 + i \frac{4}{\omega}; \quad (34)$$

and

$$\epsilon_h = \epsilon_{h0} + i \frac{\sigma_h}{\omega}; \quad (35)$$

where  $i$  is the imaginary unit,  $\epsilon_{i0}$  and  $\epsilon_{h0}$  are the dielectric constants of the inclusion and the host, and  $\sigma_i$  and  $\sigma_h$  are their conductivities, assumed frequency-independent. The time-averaged forces are now calculated from the generalization of eq. (26) to finite frequencies, namely, eq. (29).

We have chosen to use parameters given by Ref. [15], in a recent experimental study. These are listed in Table II. However, as discussed further below, it is possible that the experimentally measured forces include effects beyond the purely electrostatic interactions included in our model (such as spatially dependent conductivities of the host fluid). Therefore, our numerical results should again be considered as model calculations, not necessarily applicable to the specific experiments of Ref. [15]. In all cases, we assume that the two spherical inclusions are identical, with a dielectric constant and conductivity characteristic of SrTiO<sub>3</sub>. For the host fluid, we have considered the various materials used in the measurements of Ref. [15]. (In practice, the nonzero conductivity of SrTiO<sub>3</sub> has negligible effect on force; we have checked this by recalculating the forces with the conductivity set equal to zero, and obtained the same results.)

In Fig. 5 (a) and (b), we show the radial component of the calculated time-averaged force on a sphere of SrTiO<sub>3</sub> at  $R$  in the parallel and perpendicular geometries, for the host materials of silicone oil and castor oil. In both cases, we assume spheres of radius  $a = 3.15 \text{ mm}$ , intersphere spacing  $d = 0.01 \text{ mm}$  and applied electric field  $E_0 = 25.2 \text{ V/mm}$ , as in Ref. [15]. The magnitude of force decreases with increasing frequency, but rapidly converges to a constant value in both cases. The sign of the force is negative in (a), corresponding to an attractive force, and positive (repulsive) in (b).

If these were strictly dipole-dipole forces, the time-averaged force on the sphere at  $R$  would be given by the generalization of eq. (33) to complex dielectric functions and  $\epsilon_h \neq 1$ , namely

$$F_{av;12}^{\text{dip};?} = \frac{1}{2} F_{av;12}^{\text{dip};k} = \frac{3}{2R^4} a^6 E_0^2 \text{Re} \left[ \frac{\epsilon_i - \epsilon_h}{\epsilon_i + 2\epsilon_h} \right]^2 \epsilon_h; \quad (36)$$

Thus, in particular, the magnitude of the force in the parallel case would be twice as large as that in the perpendicular case, as in our previous examples. However, in Fig. 5, this force ratio is about 50. This difference occurs, as in Fig. 2, because of the very small separation



( $\ell = 0.01\text{ mm}$ ), which corresponds to a very short-ranged interaction. In the long range limit ( $R \gg \ell$ ), our calculated magnitude ratio agrees well with the dipole-dipole prediction, as discussed further below. This short-distance deviation from dipole-dipole forces is similar to that seen in Figs. 2{4.

Fig. 5 also shows that there is a substantial difference between the forces for silicone oil and castor oil hosts. This difference is due almost entirely to the difference in the static dielectric constants of these two hosts: the effect of the finite conductivity disappears by about 10 Hz in both cases, whereas the difference between the forces persists to much higher frequencies.

The calculated time-averaged force between spheres of  $\text{SrTiO}_3$  in a silicone oil host is plotted versus separation in Fig. 6 at a frequency of 50 Hz. In order to see the effects of a finite host conductivity, we include this conductivity in Figs. 6 (a) and 6 (b) but not in 6 (c) or 6 (d). We also set the conductivity of the sphere equal to zero in (c) and (d). Clearly, the host conductivity has very little influence on the forces at this frequency. For comparison, we also show the forces as calculated in the dipole-dipole approximation. As can be seen, there is very little difference between the two except for  $R < 1.5\text{ cm}$ . Even at such small spacings, the deviation from the dipole-dipole force is much larger for the parallel than the perpendicular configuration. At a spacing of  $0.01\text{ mm}$ , the calculated ratio of force magnitudes in the parallel and perpendicular configurations exceeds a factor of 100.

At sufficiently high host conductivity, our model predicts that the force between spheres changes sign as a function of frequency. This trend is shown in Fig. 7 for a separation of  $\ell = 0.01\text{ mm}$  between spheres. The host materials used here are ethyl benzoate, ethyl salicylate, and methyl salicylate, all of which have much greater conductivities than silicone oil. The sign change is due mainly to the greater conductivities, not the differences in static dielectric constants. To check this point, we recalculated the points of Fig. 7 assuming the same value of the real part of the dielectric constant for all three host materials; we found that the time-averaged forces changed sign at the same frequencies as in Fig. 7. Mathematically, the origin of the sign change is, of course, the dependence of the variables in eqs. (3) and (29) on the host conductivity.

The time-averaged force for this separation ranges from about  $+1.5$  to  $-1.5$  dynes for the parallel case, depending on the frequency, and from about  $+0.5$  to  $-3.0$  dynes for the perpendicular case. At high frequencies, the force approaches  $-1.0$  dyne for the parallel case,

whatever the host fluid is, and approaches a much smaller magnitude in the perpendicular case. The ratio of these forces differs greatly from the predictions of the dipole-dipole interaction, as expected for such a small separation. At very low frequencies, however, the force ratio appears to approach the dipole-dipole prediction.

Fig. 8 shows the frequency dependence of the time-averaged force between two spheres of  $\text{SrTiO}_3$  for silicone oil and  $\text{N}_2$  hosts. Both the spacings between the two spheres and the electric field  $E_0$  are larger than those for Fig. 5; they are given in the legends of each Figure. We chose these values for the parameters because they are used in the measurements of Ref. [15]. Evidently, the force between the two spheres is stronger when the two spheres are immersed in a liquid host than in a gas, all the other parameters of the forces being held constant. This behavior can be understood even in the dipole-dipole limit: it is due to the dependence of the force on  $\eta$  as in eq. (36). Also, the low-frequency forces in Fig. 8 (a) and (b) and especially (c) and (d) depend more weakly on frequency than those in Fig. 5. Another point is that, even though the intersphere spacing has been increased to 0.10 and 0.30 mm in these calculations, the calculated forces are still far from the dipole-dipole limit. Specifically, the ratio of the force magnitudes in the parallel and perpendicular geometries greatly exceeds the factor of two expected in the dipole-dipole limit. However, this ratio is smaller than that of Fig. 5, presumably because the intersphere separations are larger than in that Figure.

#### IV . D I S C U S S I O N

The present work permits calculation of electrical forces in ER fluids in a concise closed form, which permits inclusion of all multipoles and all many-body forces in a simple way. In our approach, the forces do not need to be calculated as numerical derivatives; instead, we give explicit analytical expressions for these derivatives, in terms of a pole spectrum which characterizes the microgeometry of the material. The explicit form for the derivatives is somewhat reminiscent of the Hellmann-Feynman description of quantum-mechanical forces in electronic structure theory, but differs from it in the important respects.

One striking feature of the present formalism is that it allows for the calculation of frequency-dependent forces in a simple closed form. Although such forces have been discussed in previous work [10, 11, 22, 24], the present approach is relatively simple and more

general, and places both zero and finite frequency forces within the same formalism. In our numerical work, we find that these forces can even change sign as a function of frequency. Such frequency-dependence is, of course, also present in the long-range (dipole-dipole) limit treated by others in the previous work, but it is even more apparent in the present study.

Although in the present work calculations have been carried out explicitly for two-body interaction, they can readily be extended to three-body (or multi-body) forces. The general equation (26) or (29) can be used to find the force on a sphere, no matter how many particles are contained in the suspension. Indeed, such multi-body forces are very likely to play important roles in dense suspensions, where they could possibly lead to "bond-angle-dependent" forces analogous to angle dependent interatomic elastic forces in liquid and solid semiconductors. Likewise, the calculations could be readily extended to more complex particles (e.g., hollow spherical shells), and to non-spherical particles, provided that the requisite pole spectra and matrix elements can be calculated. Also, although we have restricted our calculations in this paper to the radial component of the interparticle forces, other components can be straightforwardly computed. Finally, the present formalism can be immediately extended to the important case of magnetorheological fluids. For such fluids, eq. (26) or (29) for the force would continue to be valid, provided that  $\epsilon_i$  and  $\epsilon_h$  are replaced by  $\mu_i$  and  $\mu_h$ .

Our calculated frequency-dependent forces, obtained using parameters quoted for  $\text{SrTiO}_3$  spheres in a conducting host, may appear to disagree with those obtained in Ref. [15] at close spacing. One possible explanation for this discrepancy is that the host fluid does not exhibit its usual bulk conductivity when two highly polarizable spheres are placed in it in close proximity. Instead, there could well be non-linear screening effects of the Debye-Huckel type [40], which would mean that the picture of a two-component composite is simply not appropriate in this regime. In support of this hypothesis, we note that the reported experimental forces are still frequency-dependent at high frequencies, while the complex dielectric functions of both host and sphere should be nearly frequency-independent in this regime, leading to a frequency-independent force in this range.

The present method could readily be combined with standard molecular dynamics approaches to compute dynamical properties of electrorheological (or magnetorheological) fluids. Specifically, one could carry out molecular dynamics (MD) calculations, following the approach of several authors [5, 41, 42, 43, 44]. In such approaches, the force on a given

sphere is typically expressed as the sum of a hard-sphere repulsion, a viscous force, and an electrostatic force. The first two of these forces would be the same as in the previous MD studies, but the third would be calculated using the present method, rather than the dipole-dipole force generally used in most other MD studies. It would be of great interest to see how such quantities as viscous relaxation time would be affected by using our forces in these calculations. In addition to such calculations, one could study minimum-energy configurations of dielectric suspensions in an applied electric field, based on the forces calculated using the methods outlined here. Many such studies can already be found in the literature (see, e.g., Ref. [45] or [46]). It would be of interest to extend the present approach to calculating minimum-energy configurations including non-dipolar forces, as outlined in the present work.

#### V. ACKNOWLEDGMENTS

This work was supported by NSF Grants DMR 01-04987 and DMR 04-13395 (KK and DS). The work of DJB and XL was supported, in part, by grants from the US-Israel Binational Science Foundation and the Israel Science Foundation. The work of XL was also supported by a grant from the Sackler Institute of Solid State Physics of Tel Aviv University. All the calculations were carried out on the P4 Cluster at the Ohio Supercomputer Center, with the help of a grant of time.

- 
- [1] For reviews, see, e.g., T. Hao, *Adv. Mater.* **13**, 1847 (2001); M. Parthasarathy and D. J. Klingenberg, *Mat. Sci. Eng. R* **17**, 57 (1996); T. C. Halsey, *Science* **258**, 761 (1992); or A. P. Gast and C. F. Zukoski, *Adv. Colloid and Interface Sci.* **30**, 153 (1989).
  - [2] D. J. Hartsock, R. F. Novak, and G. J. Chaundy, *J. Rheol.* **35**, 1305 (1991).
  - [3] R. Stanway, J. L. Sproston, and J. K. E. W. Ahmed, *Smart Materials and Structures* **5**, 464 (1996).
  - [4] See, e.g., J. M. Ginder and L. C. Davis, *Appl. Phys. Lett.* **65**, 3410 (1994); M. M. Moebi, N. Jamasbi, and J. Liu, *Phys. Rev. E* **54**, 5407 (1996); B. F. Spencer, S. J. Dyke, M. K. Sain, and J. D. Carlson, *J. Eng. Mech. ASCE* **123**, 230 (1997).
  - [5] D. J. Klingenberg, F. van Swol, and C. F. Zukoski, *J. Chem. Phys.* **94**, 6170 (1991). See also

- D. J. Klingenberg, F. van Swol, and C. F. Zukoski, *J. Chem. Phys.* **94**, 6160 (1991) for similar studies in the point dipole approximation.
- [6] Y. Chen, A. F. Sprecher, and H. Conrad, *J. Appl. Phys.* **70**, 6796 (1991).
  - [7] L. C. Davis, *Appl. Phys. Lett.* **60**, 319 (1992).
  - [8] L. C. Davis, *J. Appl. Phys.* **81**, 1985 (1997).
  - [9] R. Tao, Q. Jiang, and H. K. Sim, *Phys. Rev. E* **52**, 2727 (1995).
  - [10] X. Tang, C. Wu, and H. Conrad, *J. Appl. Phys.* **78**, 4183 (1995).
  - [11] X. Tang, C. Wu, and H. Conrad, *J. Rheol.* **39**, 1059 (1995).
  - [12] B. Khusid and A. Acrivos, *Phys. Rev. E* **52**, 1669 (1995).
  - [13] H. J. H. Clercx and G. Bossis, *Phys. Rev. E* **48**, 2721 (1993).
  - [14] W. Wen and K. Lu, *Appl. Phys. Lett.* **68**, 3659 (1996).
  - [15] Z. Wang, R. Shen, X. Niu, K. Lu, and W. Wen, *J. Appl. Phys.* **94**, 7832 (2003). See also Z. Wang, Z. Peng, K. Lu, and W. Wen, *Appl. Phys. Lett.* **82**, 1796 (2003).
  - [16] D. J. Jeffrey, *Proc. Royal Soc. London A* **335**, 355 (1973).
  - [17] K. W. Yu and J. T. K. Wan, *Computer Phys. Commun.* **129**, 177 (2000).
  - [18] R. C. McPhedran and D. R. McKenzie, *Proc. Royal Soc. London A* **359**, 45 (1978).
  - [19] W. M. Suen, S. P. Wong, and K. Young, *J. Phys. D* **12**, 1325 (1979).
  - [20] J. M. Gerardy and M. Ausloos, *Phys. Rev. B* **25**, 4204 (1982).
  - [21] L. Fu, P. B. Macedo, and L. Resca, *Phys. Rev. B* **47**, 13818 (1993).
  - [22] L. C. Davis, *J. Appl. Phys.* **72**, 1334 (1992).
  - [23] F. Claro and R. Rojas, *Appl. Phys. Lett.* **65**, 2743 (1994).
  - [24] H. Ma, W. Wen, W. Y. Tam, and P. Sheng, *Phys. Rev. Lett.* **77**, 2499 (1996).
  - [25] D. J. Bergman, *Phys. Rep.* **43**, 377 (1978).
  - [26] D. J. Bergman, *Phys. Rev. B* **19**, 2359 (1979).
  - [27] D. J. Bergman, *J. Phys. C : Solid State Physics* **12**, 4947 (1979).
  - [28] A review of the spectral method for composite media appears in D. J. Bergman and D. Stroud, *Solid State Physics* **46**, 147 (1992); a more modern version of this method appears in Ref. [29]; a modern version with computational capabilities for any periodic microgeometry is described in Ref. [30].
  - [29] D. J. Bergman, *SIAM J. Appl. Math.* **53**, 915 (1993).
  - [30] D. J. Bergman and K.-J. Dunn, *Phys. Rev. B* **45**, 13262 (1992).

- [31] J. P. Huang, Chem. Phys. Lett. 390, 380 (2004).
- [32] T. C. Halsey and W. Toor, Phys. Rev. Lett. 65, 2820 (1990).
- [33] R. Tao and J. M. Sun, Phys. Rev. Lett. 67, 398 (1991).
- [34] R. Tao and J. M. Sun, Phys. Rev. A 44, R 6181 (1991).
- [35] H. Hellmann, Einführung in die Quantenchemie (F. Deuticke, Leipzig, 1937), p. 285; R. P. Feynman, Phys. Rev. 56, 340 (1939).
- [36] G. Kresse and J. Hafner, Phys. Rev. B 47, R 558 (1993); G. Kresse and J. Hafner, Phys. Rev. B 49, 14251 (1994).
- [37] Y. Kantor and D. J. Bergman, J. Phys. C : Solid State Physics 15, 2033 (1982).
- [38] Specifically, when the spheres are moved at fixed potential on the boundaries, the energy  $W$  of the system changes. However, the batteries which hold the potential fixed supply twice as much energy to the system as the change in  $W$ . For a discussion of differences between force calculations at fixed potential and fixed charge, see, e. g., J. D. Jackson, Classical Electrodynamics, 3rd ed. (Wiley, New York, 1999), pp. 167{169.
- [39] M. Galassi, J. Davies, J. Theiler, B. Gough, G. Jungman, M. Booth, and F. Rossi, GNU Scientific Library, 1.5 ed. (GSL Team, 2004).
- [40] P. Debye and E. Huckel, Phys. Z. 24, 185, 305 (1923).
- [41] R. T. Bonnecaze and J. F. Brady, J. Chem. Phys. 96, 2183 (1992).
- [42] D. J. Klingenberg, F. van Swol, and C. F. Zukoski, J. Chem. Phys. 91, 7888 (1989).
- [43] K. C. Hass, Phys. Rev. E 47, 3362 (1993).
- [44] R. Tao and Q. Jiang, Phys. Rev. Lett. 73, 205 (1994).
- [45] L. C. Davis, Phys. Rev. A 46, R 719 (1992).
- [46] See, e. g. Z. D. Cheng, W. B. Russel, and P. M. Chaikin, Nature 401, 893 (1999).

# TABLES

R (cm)	Force ratio	(R/2a)=(2a/R)
0.630	602.3	0.0000
0.631	88.5	0.0016
0.632	52.5	0.0032
0.633	38.8	0.0048
0.634	31.5	0.0063
0.635	26.8	0.0079
0.636	23.5	0.0095
0.637	21.1	0.0111
0.638	19.2	0.0127
0.639	17.7	0.0143
0.640	16.5	0.0159

TABLE I. The ratios of the magnitudes of the forces between two identical spheres in the parallel and perpendicular configurations, calculated at several small separations and assuming  $\epsilon_i = 10^5$ ,  $\epsilon_h = 1$ ,  $a = 3.15\text{ mm}$ ,  $E_0 = 25.2\text{ V/mm}$ , and  $\theta = 0$ . The force is attractive in the parallel configuration, repulsive in the perpendicular configuration.

Material	Dielectric constant	Conductivity
SrTiO <sub>3</sub>	249.0	$2.0 \cdot 10^8$
Silicone oil	2.54	$1.0 \cdot 10^{13}$
Castor oil	4.20	$1.0 \cdot 10^{13}$
Ethylbenzoate	5.45	$5.0 \cdot 10^8$
Ethylsalicylate	8.65	$1.0 \cdot 10^7$
Methylsalicylate	9.46	$6.0 \cdot 10^7$
N <sub>2</sub> gas	1.00058	0

TABLE II. Parameters for the calculations shown in Figs. 5-8. The columns denote the material, the real part of its dielectric constant, and its conductivity (in S/m). All except for SrTiO<sub>3</sub> are used as host materials in the suspensions.

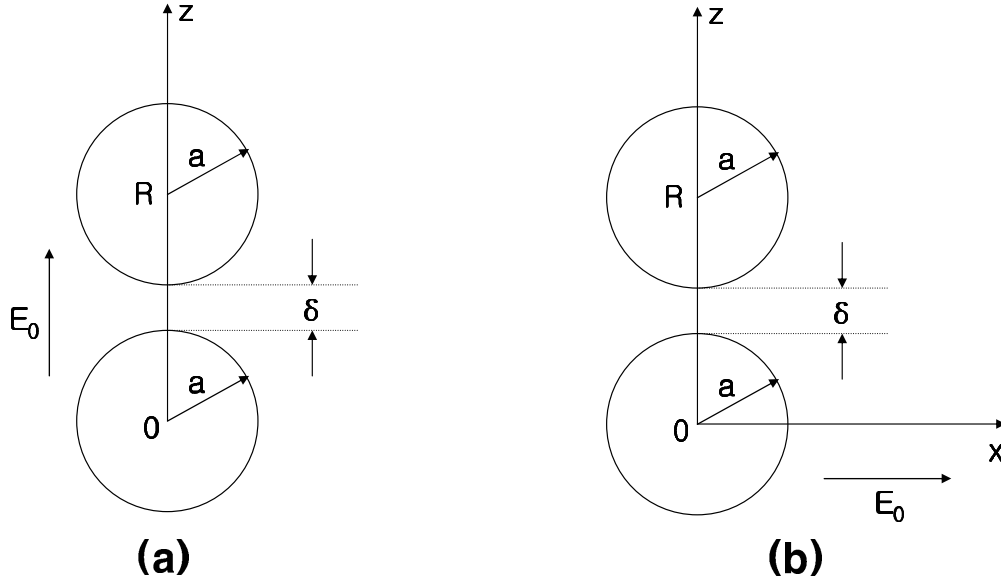


FIG .1: Geometry considered in most of our calculations: Two identical spheres of radius  $a$  are located at the origin and at  $z = R$ , and are contained in a host material.  $\delta$  is the surface-to-surface distance between the two spheres. The complex dielectric function of the spheres is  $\epsilon_i(\omega)$  and that of the host material is  $\epsilon_h(\omega)$ . A spatially uniform electric field is applied in the  $z$  direction in (a) and in the  $x$  direction in (b).

FIGURES



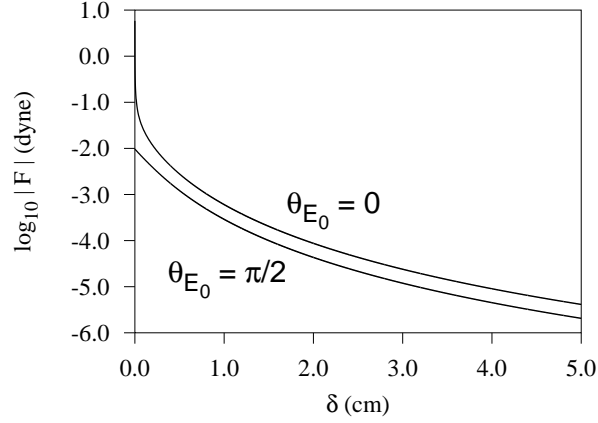


FIG . 2: Magnitude of the radial component of the force at zero frequency between two identical spheres of radius  $a$ , with  $\epsilon_i = 10^5$ ,  $\epsilon_h = 1$ , plotted as a function of sphere separation, for electric field parallel to axis between spheres ( $\theta_{E_0} = 0$ ), and field perpendicular to that axis ( $\theta_{E_0} = \pi/2$ ). Note the logarithmic scale on the vertical axis. In both cases, we assume sphere radii of  $3.15 \text{ mm}$ , and an electric field of strength  $25.2 \text{ V/mm}$ , as in Ref. [15]. The force in the parallel field case is negative (attractive) while that in the perpendicular field case is positive (repulsive). In this and the following two plots, the force is calculated at zero frequency.

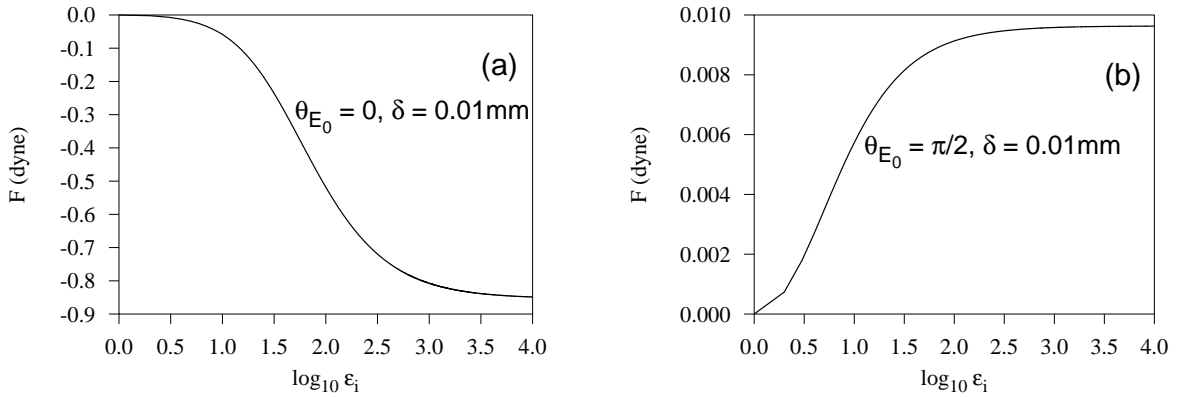


FIG . 3: The radial component of the force at zero frequency between two identical spheres of dielectric constant  $\epsilon_i$ , radius  $a = 3.15 \text{ mm}$ , in a host of dielectric constant  $\epsilon_h = 1$ , at an intersphere spacing (surface-to-surface separation) of  $0.01 \text{ mm}$ , plotted as a function of  $\epsilon_i$ , for (a) electric field parallel to the axis between spheres, and (b) field perpendicular to that axis. We assume an electric field of strength  $25.2 \text{ V/mm}$ . Negative and positive forces denote attractive and repulsive forces, respectively.

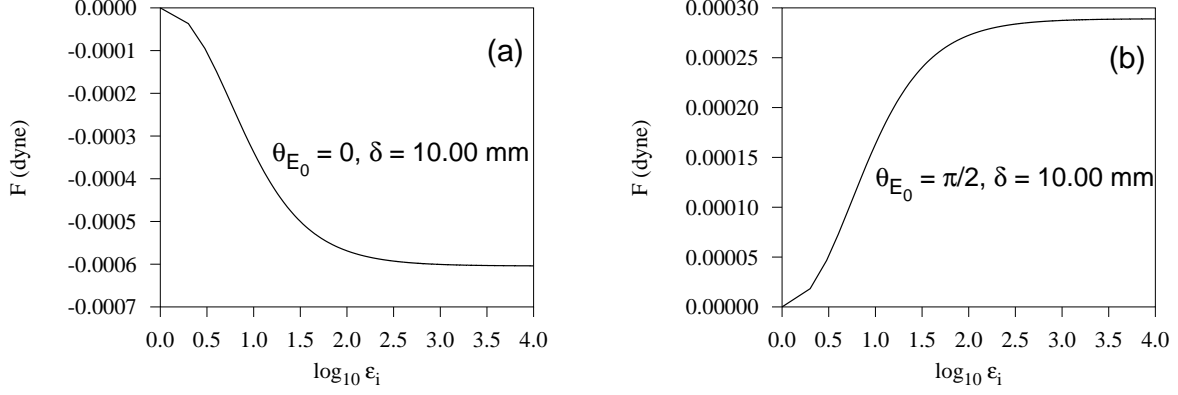


FIG . 4: Same as Fig. 3, but for an intersphere spacing  $\delta = 10.00$  mm .

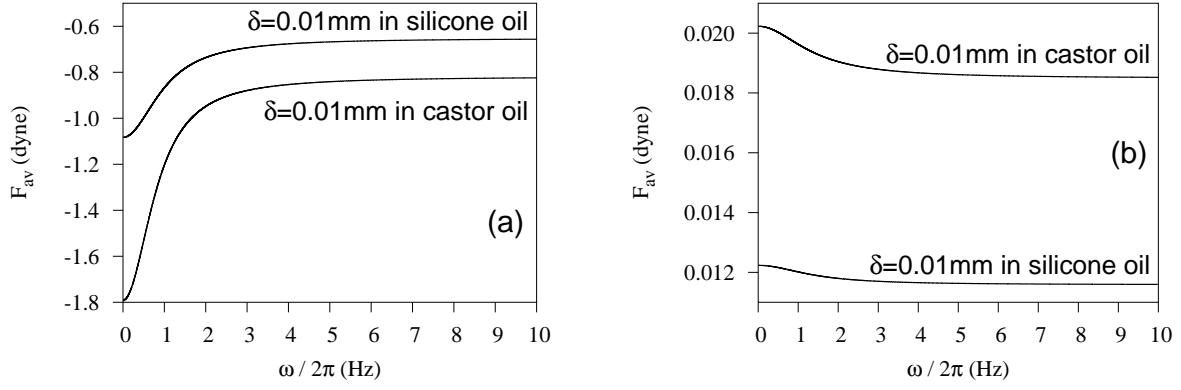


FIG . 5: The radial component of the time-averaged force between two identical spheres of  $\text{SrTiO}_3$ , plotted as a function of frequency for the host materials of silicone oil and castor oil, respectively. For both cases we use  $\delta = 0.01$  mm ,  $a = 3.15$  mm , and  $E_0 = 25.2$  V/mm . The electric field is parallel to the line connecting the spheres in (a) and perpendicular to that line in (b) . A negative value denotes an attractive force.

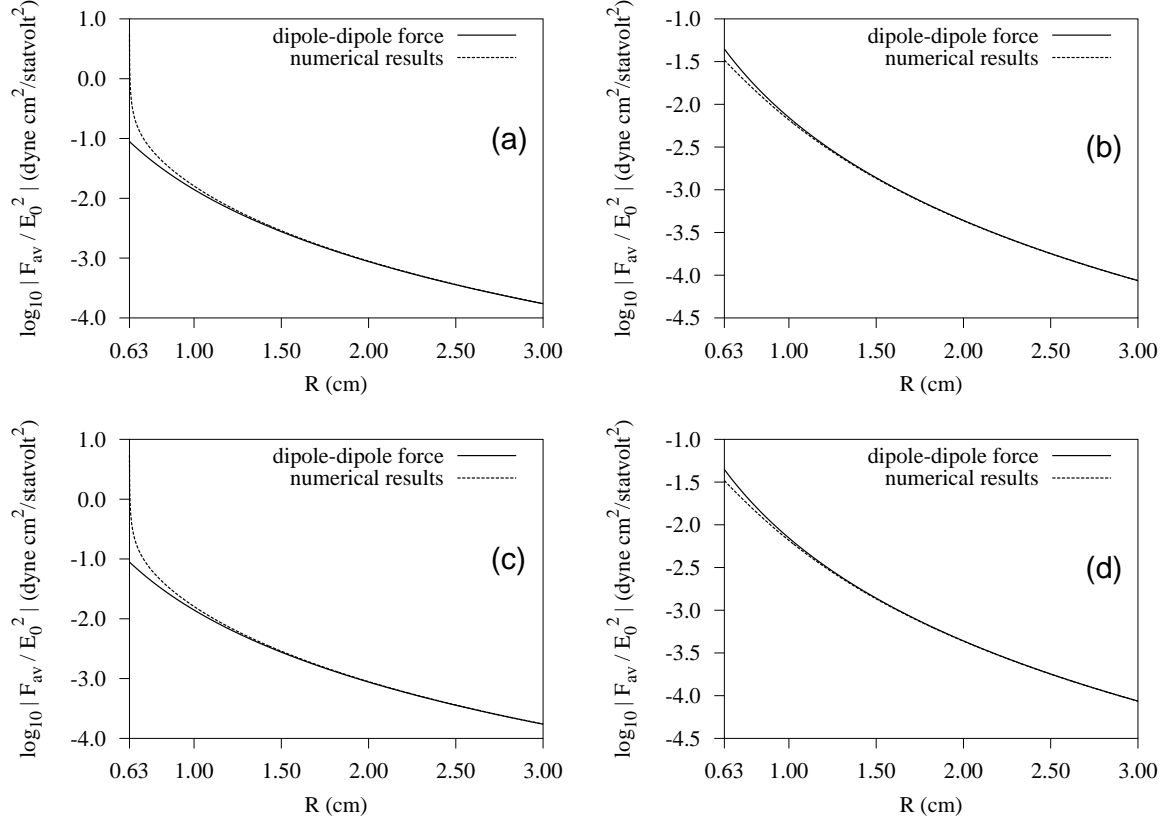


FIG . 6: (a) and (b) : Magnitude of the radial component of the time-averaged force between two identical spheres of  $\text{SrTiO}_3$ , divided by  $E_0^2$ . Also plotted is the corresponding quantity in the dipole-dipole approximation. Both are plotted on logarithmic scale as a function of separation  $R$  for a host material of silicone oil and a fixed frequency of 50 Hz. The spheres have radii 3.15 mm. The electric field is parallel to the line between the two spheres in (a) and perpendicular to that line in (b). (c) and (d) : Same as (a) and (b) except that the conductivities of the spheres and the host are set equal to zero in these calculations. The forces are attractive in (a) and (c), repulsive in (b) and (d).

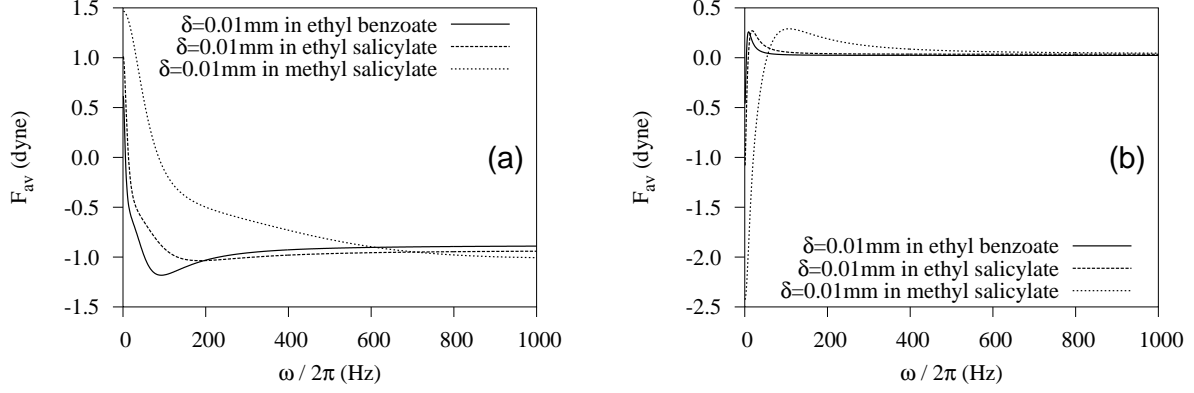


FIG .7: The radial component of the time-averaged force between two identical spheres of  $\text{SrTiO}_3$  separated by  $R$ , plotted as a function of frequency for the host materials of ethyl benzoate, ethyl salicylate, and methyl salicylate, respectively. The electric field is parallel to the line connecting the two spheres in (a) and perpendicular to that line in (b). In all cases,  $\delta = 0.01\text{mm}$ ,  $a = 3.15\text{mm}$ , and  $E_0 = 25.2\text{V/mm}$ .

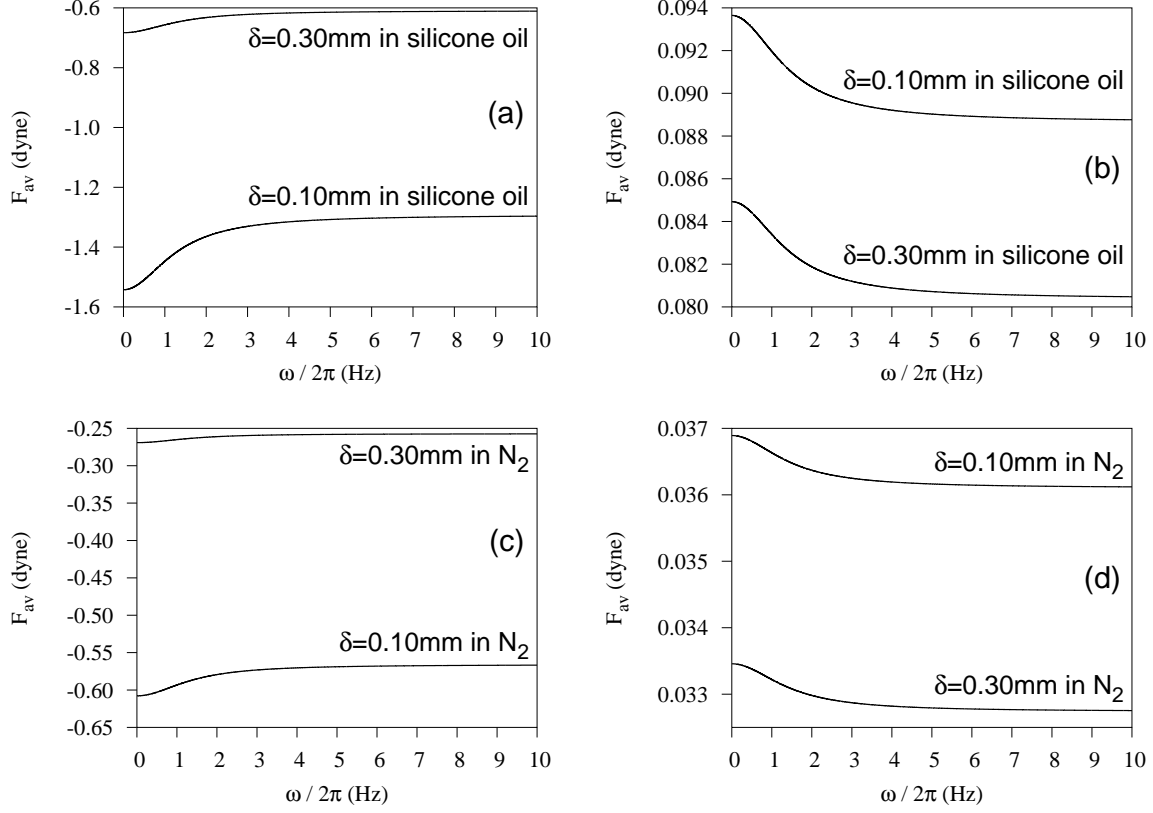


FIG .8: The radial component of the time-averaged force between two identical spheres of  $SrTiO_3$  separated by  $R$ , plotted as a function of frequency for host materials consisting of silicone oil [(a) and (b)] and  $N_2$  [(c) and (d)], with gap spacings  $\delta = 0.10$  mm and  $\delta = 0.30$  mm. The applied electric field is  $E_0 = 71.3$  V/mm and  $a = 3.15$  mm for all the cases. The electric field is parallel to the line between two spheres in (a) and (c) and perpendicular to that line in (b) and (d).